

This is the submitted version of the following article: Puyuelo, B., Gea, T. and Sánchez, A. *GHG emissions during the high-rate production of compost using standard and advanced aeration strategies* in Chemosphere (Ed. Elsevier), vol. 109 (Aug. 2014), p. 64-70, which has been published in final form at DOI 10.1016/j.chemosphere.2014.02.060

© 2014. This manuscript version is made available under the CC-BY-NC-ND 4.0 license <http://creativecommons.org/licenses/by-nc-nd/4.0/>

1 **GHG emissions during the high-rate production of compost using standard and**  
2 **advanced aeration strategies**

3  
4  
5 B. Puyuelo, T. Gea, A. Sánchez\*

6  
7  
8 Composting Research Group

9 Department of Chemical Engineering

10 Escola d'Enginyeria, Universitat Autònoma de Barcelona

11 08913-Bellaterra (Cerdanyola del Vallès, Barcelona, Spain)

12  
13 \*Corresponding author:

14 Dr. Antoni Sánchez

15 Phone: 34- 935811019

16 Fax: 34- 935812013

17 E-mail address: antoni.sanchez@uab.cat

18

19

20 **Abstract**

21           In this study, we have evaluated different strategies for the optimization of the  
22 aeration during the active thermophilic stage of the composting process of source-  
23 selected organic fraction of municipal solid waste (or biowaste) using reactors at bench  
24 scale (50 L). These strategies include: typical cyclic aeration, oxygen feedback  
25 controller and a new self-developed controller based on the on-line maximization of the  
26 oxygen uptake rate (OUR) during the process. Results highlight differences found in the  
27 emission of most representative greenhouse gases (GHG) emitted from composting  
28 (methane and nitrous oxide) as well as in gases typically related to composting odor  
29 problems (ammonia as typical example). Specifically, the cyclic controller presents  
30 emissions that can double that of OUR controller, whereas oxygen feedback controller  
31 shows a better performance with respect to the cyclic controller. A new parameter, the  
32 respiration index efficiency, is presented to quantitatively evaluate the GHG emissions  
33 and, in consequence, the main negative environmental impact of the composting  
34 process. Other aspects such as the stability of the compost produced and the  
35 consumption of resources are also evaluated for each controller.

36

37

38 **Keywords:** Composting; Aeration control; Oxygen uptake rate; Greenhouse gases  
39 emissions; Respiration efficiency.

40

## 41 **1. Introduction**

42 Aeration is a fundamental factor to ensure the aerobic conditions during the  
43 composting process. It aims to maintain an optimal biological activity and also it is a  
44 critical parameter on the gaseous emissions of  $\text{NH}_3$ ,  $\text{N}_2\text{O}$ ,  $\text{CH}_4$  and Volatile Organic  
45 Compounds (VOCs) (Haug, 1993; Smet et al., 1999). Therefore, the aeration is a key  
46 parameter in the study of environmental impact categories commonly used in waste  
47 management Life Cycle Assessment such as Global Warming Potential (GWP), which  
48 refers to warming potential of different gases related to carbon dioxide. The main  
49 related substances emitted during composting related to the study of GWP are  $\text{NH}_3$ ,  
50  $\text{N}_2\text{O}$  and  $\text{CH}_4$ . It is necessary to minimize these emissions to protect the environment  
51 and the human health (European Directive 2008/1/CE).

52 Today, there are different strategies that use forced aeration for the high-rate  
53 production of compost from several organic wastes. In general, industrial facilities  
54 usually provide air to the organic matrix from predefined time cycles. Another typical  
55 system is the oxygen feedback controller that provides a preset airflow as a function of  
56 the oxygen content of exhaust gases. In other cases, the airflow is supplied as a function  
57 of the mass temperature, although this technique does not guarantee the prevalence of  
58 aerobic conditions. Some recent studies have proposed other strategies based on  
59 complex models of the process (Papadimitriou et al., 2010; Giusti et al., 2010). These  
60 can be defined as promising strategies but the implementation of these systems can be  
61 difficult and costly at industrial scale. A recent study proposed a new controller based  
62 on the oxygen uptake rate (OUR) evolution (Puyuelo et al., 2010). This OUR controller  
63 avoids the current limitations of the typical systems such as airflow fluctuation, the

64 definition of optimal oxygen and/or temperature set-points or even the definition of  
65 suitable airflow levels.

66         Also, the aeration strategy used influences gaseous emissions generated during  
67 composting. Osada et al. (2000) demonstrated that a high airflow decreased the CH<sub>4</sub> and  
68 N<sub>2</sub>O emissions due to the minimization of anaerobic zones in their studies on slurry  
69 composting. This phenomenon was also observed by Fukumoto et al. (2003), although  
70 they observed an increase in the NH<sub>3</sub> emissions, in agreement with other authors (de  
71 Guardia et al., 2008; Kim and Deshusses, 2008; Shen et al., 2011). Suitable oxygen  
72 content in composting mass would limit the formation of anaerobic zones avoiding the  
73 generation of intermediate products of the anaerobic metabolism (Scaglia et al., 2011).  
74 Other studies have concluded that, when comparing continuous and intermittent  
75 aeration, the former reduces the greenhouse gases (GHG) emissions associated to the  
76 composting process (Keener et al., 2001).

77         Accordingly, the main objective of this work is to determine and compare the  
78 cumulative emissions of NH<sub>3</sub>, N<sub>2</sub>O and CH<sub>4</sub> obtained with different forced aeration  
79 strategies, which are an oxygen feedback controller, cyclic aeration (not closed-loop)  
80 and a new novel controller developed in a previous work (OUR controller, Puyuelo et  
81 al., 2010). All emissions values are expressed per Mg of waste treated. Nevertheless, a  
82 more specific unit is included (known as RIE: Respiration Index Efficiency), in which  
83 the process efficiency is also considered (Colón et al., 2012) to take into consideration  
84 the stabilization degree achieved in the process. Finally, the GWP associated to each  
85 controller together with the energy requirements are also determined. These results are  
86 expressed as kg CO<sub>2</sub>-eq Mg<sup>-1</sup> (of waste treated) and RIE units.

87

## 88 **2. Materials and methods**

### 89 *2.1. Composting material*

90 The waste used in all experiments was source-selected Organic Fraction of  
91 Municipal Solid Waste (OFMSW) mixed with pruning waste as a bulking agent  
92 (volumetric ratio 1 to 1) collected in a composting plant located in Manresa (Barcelona,  
93 Spain).

94 A total amount of 200 kg was collected to carry out the three experiments and  
95 replications with the same material. After collection, a homogeneous sample was used  
96 for waste characterization and all the remaining waste was frozen at -18 °C. Before  
97 starting-up each composting experiment, the material was removed from the freezer and  
98 thawed in the laboratory at room temperature for 24 h. No more than three months were  
99 necessary to undertake the experiments so it was considered that freezing did not  
100 perturb the biological activity of the waste (Pognani et al., 2011).

101

### 102 *2.2. Composting reactors*

103 The complete description and the scheme of the composting reactors can be  
104 found at Puyuelo et al. (2010). They were adiabatic cylindrical reactors with an  
105 operating volume of 50 L. Approximately 25 kg of the waste selected were treated in  
106 each experiment. Two geometrically identical reactors were used in parallel. The reactor  
107 walls were thermally isolated with polyurethane foam in order to avoid heat losses. A  
108 perforated plate was fitted into the bottom of the reactor to support the material, to help  
109 leachate removal and to optimize the airflow circulation. Two orifices were situated at  
110 the bottom cover of the reactor, one to introduce air from a compressor and other for  
111 leachate removal. Two more orifices were situated at the top cover. One hole was to

112 insert the Pt-100 sensor for temperature monitoring (Desin Instruments, Barcelona,  
113 Spain), which was placed at middle height of the material matrix. The other orifice was  
114 used to remove the exhaust gases in order to analyze the oxygen concentration. Before  
115 the oxygen sensor (Xgard, Crown, UK) a water trap by refrigeration was placed to avoid  
116 wet gases passing through the gas analyzer.

117 The data acquisition and control system was composed by an acquisition chassis  
118 (cDAQ-9172, National Instruments, USA) connected to a PC and using LabView 8.6  
119 software (National Instruments, USA). Temperature, outgoing oxygen gas  
120 concentration, and inlet airflow were the parameters monitored during the experimental  
121 trials. Temperature probe and oxygen sensor were connected to the data acquisition  
122 chassis. Instead, the input and output electrical signals of the flow meter were directly  
123 connected to the PC through an RS-232 serial port. All the data were recorded and  
124 shown in a graph or in the program interface from which different control systems could  
125 be programmed.

126

### 127 *2.3. Airflow strategies and control*

128 Three different strategies to regulate the inlet airflow were studied and  
129 compared. Two different closed-loop controllers and a third system based on a cycled  
130 on-off aeration configuration were tested. The lowest airflow applied to the reactor was  
131 never below  $0.2 \text{ L min}^{-1}$  ( $2 \cdot 10^{-2} \text{ L min}^{-1} \text{ kg}^{-1} \text{ DM}$ , Dry Matter) to overcome an excessive  
132 pressure drop of the reactor and to obtain a constant gas flow for oxygen monitoring  
133 purposes. The highest flow depended on each system (details below). All experiments  
134 were running for 20 d until the OUR was always below  $1 \text{ g O}_2 \text{ g}^{-1} \text{ OM h}^{-1}$  (Organic

135 Matter) and therefore, it was assumed that most of the easily biodegradable material had  
136 been degraded.

137

### 138 2.3.1. Oxygen feedback control

139 This controller was based on the airflow manipulation by means of the oxygen  
140 content measured in the exhaust gas. Oxygen set point was fixed at  $12\pm 0.5\%$  (Ruggieri  
141 et al., 2008). Simulating the controllers used at industrial facilities, the system applied a  
142 high flow for oxygen levels below 11.5% and a low flow for levels over 12.5%, whereas  
143 the controller would maintain former airflow when the measure was between 11.5 and  
144 12.5%. The predetermined flows were 3 and  $0.2 \text{ L min}^{-1}$  ( $3.5 \cdot 10^{-1}$  and  $2 \cdot 10^{-2} \text{ L min}^{-1} \text{ kg}^{-1}$   
145  $\text{DM}$ ). The airflow-equivalent has been calculated as the average air forced into the  
146 system for a period of 6 h, to better illustrate the controller performance in terms of  
147 graphical representation.

148

### 149 2.3.2. Cyclic airflow

150 This is the most extended system in forced-aerated composting facilities. In this  
151 case, inlet airflow was regulated automatically by predetermined timed cycles. On the  
152 basis of the study presented by Ruggieri et al. (2008), the airflow regulation was  
153 provided in cycles of 5 min at  $5 \text{ L min}^{-1}$  ( $0.4 \text{ L min}^{-1} \text{ kg}^{-1} \text{ DM}$ ) and 25 min at  $0.2 \text{ L min}^{-1}$   
154 ( $1.6 \cdot 10^{-2} \text{ L min}^{-1} \text{ kg}^{-1} \text{ DM}$ ). This is equivalent to  $1 \text{ L min}^{-1}$ .

155

### 156 2.3.3. OUR controller

157 This new control strategy has been developed, probed and validated by Puyuelo  
158 et al. (2010), given a detailed explanation on the algorithm developed. Briefly, the main



159 objective was to build an automatic airflow regulation that optimizes the biological  
160 activity, that is, that provides the maximum OUR along the process. In consequence,  
161 and taking into account the straight relation between airflow and OUR, it was defined  
162 that the system should be designed to apply the airflow that permitted the maximum  
163 possible OUR in each moment. In summary, this goal was achieved through a control  
164 system working in cycles. The system takes an action according to the comparison  
165 among OUR and flow determined in consecutive previous cycles.

166

#### 167 2.3.4. Replications

168 Three replications were carried out for the OUR controller. Two replications  
169 were conducted for the oxygen feedback and cyclic controller, respectively. In this case,  
170 there is a large number of data available in literature regarding GHG emissions from  
171 composting using these typical controllers (He et al., 2001; Pagans et al., 2006; Shen et  
172 al., 2011; Colón et al.; 2012). Figures are presented as an example of each controller  
173 due to space limitations. All the information regarding replications of each experiment  
174 conducted in this study is presented in the Supplementary Information section (Fig. S1-  
175 S4). Average and standard deviation values of some process parameters and GHG  
176 emissions are presented in Tables 2 and 3.

177

#### 178 2.4. *Parameters evaluated*

179 To evaluate quantitatively each control system, different biological, economical  
180 and environmental variables were determined that are described below. Additionally,  
181 the initial and final material stability degree was evaluated by determining the  
182 corresponding dynamic respiration index (DRI) according to the methodology described

183 by Ponsá et al. (2010). This measure was undertaken from a representative sample after  
184 mixing vigorously the initial sample collected and the final material obtained.

185

#### 186 2.4.1. OUR

187 The experimental OUR was determined from on-line empirical data on airflow  
188 and oxygen using Eq. 1, which is deduced from the mass balance in a pseudo steady-  
189 state conditions:

$$190 \quad OUR = F(0.209 - y_{O_2(LM)}) \frac{P \cdot 32 \cdot 60}{RT} \quad (1)$$

191 where: OUR (g O<sub>2</sub> h<sup>-1</sup>); F, airflow in the reactor (L min<sup>-1</sup>); y<sub>O<sub>2</sub>(LM)</sub>, is the logarithmic  
192 mean between the oxygen molar fraction in the exhaust gases and the inlet air (mol O<sub>2</sub>  
193 mol<sup>-1</sup>), since the Residence Time Residence assays demonstrated a similar pattern to  
194 plug flow (Puyuelo et al., 2010); P, pressure of the system assumed constant at 101.3  
195 kPa; 32, oxygen molecular weight (g O<sub>2</sub> mol<sup>-1</sup> O<sub>2</sub>); 60, conversion factor from minute to  
196 hour; R, ideal gas constant (8.31 kPa L K<sup>-1</sup> mol<sup>-1</sup>); T, temperature at which F is  
197 measured (K).

198

#### 199 2.4.2. Stability degree

200 DRI was measured in a respirometer built and start-up by Ponsá et al. (2010) on  
201 the basis of the methodology proposed by Adani et al. (2006) to assess the biological  
202 stability degree of an organic sample. It is expressed in mg O<sub>2</sub> g<sup>-1</sup> OM h<sup>-1</sup>.

203

#### 204 2.4.3. Energy consumption

205 The total energy consumption (E) for each experiment was estimated from the  
206 total air supplied. It was determined in kJ applying a conversion factor (396 kJ m<sup>-3</sup>) to

207 transform the total m<sup>3</sup> of air supplied into the total energy consumed by the air  
208 compressor (manufacturer's data). In addition, this parameter has also been calculated  
209 as a function of the process efficiency using a new unit proposed by Colón et al. (2012).  
210 They suggested determining the process resources consumption taking into account the  
211 yield of the process calculated as DRI reduction to provide a fair comparison in terms of  
212 stabilization of organic matter. This new unit is RIE and in this case is applied to the  
213 energy consumption (RIE<sub>ec</sub>). This measure is calculated as follows (Eq. 3):

$$214 \quad \text{RIE}_{ec} = \frac{E}{\text{DRI}_{\text{initial}} - \text{DRI}_{\text{final}}} \quad (3)$$

215 where: RIE<sub>ec</sub> is the energy consumption associated to the RIE (kJ (mg O<sub>2</sub> g<sup>-1</sup> OM h<sup>-1</sup>)  
216 <sup>1</sup>); E is the total energy consumption along the experimental time (kJ) and (DRI<sub>initial</sub>-  
217 DRI<sub>final</sub>) is the DRI reduction obtained during the experiment (mg O<sub>2</sub> g<sup>-1</sup> OM h<sup>-1</sup>).

218

#### 219 2.4.4. Determination of gaseous emissions

220 The gaseous emissions considered were CH<sub>4</sub>, N<sub>2</sub>O and NH<sub>3</sub>. These measures  
221 were undertaken off line once a day.

222

#### 223 CH<sub>4</sub> and N<sub>2</sub>O quantification: Chromatographic Methods

224 CH<sub>4</sub> and N<sub>2</sub>O analysis were undertaken by means of gas chromatography  
225 (Agilent Technologies 6890N Network GC system, Madrid, Spain). Gaseous samples  
226 were directly collected in a 1 L Tedlar bag. CH<sub>4</sub> and N<sub>2</sub>O were analyzed as stated by  
227 Colón et al. (2012). Briefly, methane was analyzed by gas chromatography using a  
228 Flame Ionization Detector (FID) and a HP-Plot Q column (30 m, 0.53 mm, 40 μm) with  
229 a detection limit of 1 ppm. The gas chromatography operation conditions were as  
230 follows: oven temperature isothermal at 60 °C, injector temperature 240 °C, FID

231 temperature 250 °C; carrier gas N<sub>2</sub> at 27.6 kPa pressure. The injected volume was 500  
232 μL and the analysis time was 4 min. Nitrous oxide was analyzed by gas chromatography  
233 using an Electron Capture Detector (ECD) and a HP-Plot Q column (30 m, 0.53 mm, 40  
234 μm) with a detection limit of 50 ppb<sub>v</sub>. The gas chromatography operation conditions  
235 were as follows: oven temperature isothermal at 60 °C, injector temperature 120 °C,  
236 ECD temperature 345 °C; carrier gas N<sub>2</sub> at 27.6 kPa pressure. The injected volume was  
237 500 μL and the analysis time was 4 min.

238

239 NH<sub>3</sub> quantification

240 Ammonia concentration was measured in-situ with an ammonia sensor (ITX  
241 T82), with a measurement range of 0 to 1200 ppm. The sensor was placed in a 1.5 L  
242 chamber with gas flowing from the reactor. The concentration measure was considered  
243 valid after reaching a stabilized value during a period of constant flow (approximately 5  
244 min).

245

246 2.4.5. Global emissions

247 From each concentration of gas and knowing the airflow associated to the  
248 measuring time, the emission rate of each component was evaluated as follows:

$$249 \quad E_x = C_x \frac{P}{RT} MW_x F \quad (4)$$

250 where: E<sub>x</sub> is the emission rate expressed as mg s<sup>-1</sup> for the pollutant considered (being x

251 CH<sub>4</sub>, N<sub>2</sub>O or NH<sub>3</sub>); C<sub>x</sub> is the concentration of each pollutant determined analytically

252 (ppm); P is the pressure in atm; MW<sub>x</sub>, is the pollutant molecular weight (g mol<sup>-1</sup>) and F

253 is the gas flow (m<sup>3</sup> s<sup>-1</sup>).

254 To transform the emissions rates in units of total mass of a contaminant produced per  
255 weight of waste treated the Eq. 5 was used:

$$256 \quad E_T = \frac{\int_0^t E_x(t) dt}{M} \quad (5)$$

257 where:  $E_T$  is the total mass of contaminant emitted per mass of the waste treated (kg  
258  $Mg^{-1}$ );  $E_x(t)$  is the emission rate determined in a time  $t$  ( $kg s^{-1}$ );  $dt$  is the time interval  
259 considered and  $M$  is the total mass of the waste treated ( $Mg$ ).

260 Similarly as it was calculated for the energy consumption, the global emissions  
261 were also determined through the unit that considers the efficiency in the stabilization  
262 process (RIE). In this case, it was calculated according to the Eq. 6.

$$263 \quad RIE_e = \frac{E_T}{DRI_{initial} - DRI_{final}} \quad (6)$$

264 where:  $RIE_e$  is associated to the global emissions of each pollutant and it is calculated as  
265 kg of gas emitted per  $Mg$  of OFMSW treated ( $E_T$ ) and per  $mg O_2 g^{-1} OM h^{-1}$  reduced  
266 during the process ( $DRI_{initial} - DRI_{final}$ ).

267

#### 268 2.4.6. GWP

269 The environmental impacts associated at each controller were determined  
270 according to the CML 2001 methodology, which was developed by the Centre of  
271 Environmental Science of Leiden University (Guinée, 2001). In this study, only the  
272 GWP category was considered to perform an overall comparison of the GHG emissions  
273 associated to the airflow control strategy. Therefore, the global emissions of  $CH_4$  and  
274  $N_2O$  were transformed to  $kg CO_2\text{-eq}$  (25 and 296  $kg CO_2\text{-eq kg}^{-1}$  contaminant,  
275 respectively) and the total mass was added to the energy consumption expressed as  $kg$

276 CO<sub>2</sub>-eq (1.068 kg CO<sub>2</sub>-eq kWh<sup>-1</sup>). CO<sub>2</sub> from biogenic sources was not considered in the  
277 GWP analysis (IPCC, 2006).

278

### 279 *2.5. Analytical methods*

280 DM, OM and total organic carbon (TOC) were determined according to the  
281 standard procedures (U.S. Department of Agriculture and U.S. Composting Council,  
282 2001).

283 Air Filled Porosity (AFP) in the reactor was measured using a self made constant  
284 volume air pycnometer connected to the reactor according to Ruggieri et al. (2009).

285 AFP is expressed as the volumetric ratio of pore filled with air to total sample volume.

286

## 287 **3. Results and discussion**

### 288 *3.1. Chemical properties of the initial and final waste*

289 The main chemical characterization of the initial OFMSW collected and the  
290 different final products obtained by means of each airflow strategy is shown in the  
291 Table 1. In general, the contents of DM, OM and TOC were considerably lower at the  
292 end of the experiments, indicating a correct performance of the composting process.

293 Instead, the nitrogen concentration increased. Although part of the nitrogen content is  
294 lost as gaseous emissions or, to a minor extent, as leachate (which were negligible in  
295 these experiments), during the aerobic metabolism the organic carbon consumption is  
296 among 20 to 30 times higher than the nitrogen biodegradation (Puyuelo et al., 2011).

297 The physical structure of the waste and bulking agent initial mixture resulted in 59% of  
298 AFP. This value was within the optimum range (30-70%) defined by Ruggieri et al.  
299 (2009) for different organic wastes.

300

### 301 *3.2. Experimental evolution*

302           Figure 1 shows the evolution of oxygen, temperature, airflow supplied and OUR  
303 for each control strategy studied. Temperatures over 50 °C were held for approximately  
304 10 d in all experiments. The starting temperature was lower in the experiment using the  
305 oxygen controller (Fig. 1a) and this provoked a slower start-up. However once  
306 temperature reached 25 °C the process performance was similar to the other  
307 experiments.

308           Cyclic aeration strategy follows a constant aeration pattern along the process that  
309 provoked low oxygen content in exhaust gases in the high-rate decomposition phase,  
310 around 5% in the period day 2 – day 6. Contrary both oxygen and OUR controllers  
311 successfully maintained oxygen levels over 10% along the process. Figure 1a shows the  
312 airflow-equivalent to illustrate the varying frequency of high-low flow alternation along  
313 the process for oxygen feedback controller. In general, the airflow evolution was the  
314 main difference observed among the controllers. All the parameters studied evolved  
315 smoothly in the experiment using the OUR controller. On the contrary, the other  
316 controllers caused continuous fluctuations hampering the biomass acclimatization and,  
317 in consequence, the process performance.

318           The main process parameters were considered for further comparison of the  
319 controllers: energy consumption,  $OUR_{max}$ , and final DRI results (Table 2). The initial  
320 DRI of the waste collected was  $5.4 \pm 0.1 \text{ mg O}_2 \text{ g}^{-1} \text{ OM h}^{-1}$ . Cyclic aeration strategy  
321 required the lowest energy consumption while oxygen and OUR controller presented  
322 similar consumptions. Oxygen controller achieved the highest  $OUR_{max}$  (15.1) when  
323 applying a constant airflow of  $3 \text{ L min}^{-1}$  and a close value (13.0) was reached in the

324 OUR controller. In a previous work, it was confirmed that during the high-rate phase,  
325 the biological activity is always the limiting step and the oxygen concentration in the  
326 biofilm is practically negligible (Puyuelo et al., 2010).

327

### 328 3.3. Gaseous emissions

#### 329 3.3.2. CH<sub>4</sub> evolution

330 CH<sub>4</sub> emissions along the composting process are a consequence of low oxygen  
331 content, which favors the anaerobic biologic activity. Normally, it is due to excessive  
332 moisture or insufficient aeration.

333 Figure 2a shows CH<sub>4</sub> profiles for each aeration strategy studied. CH<sub>4</sub> was not  
334 detected for the first 4 d in the exhaust gases. It has been recently described that the  
335 highest CH<sub>4</sub> emissions are produced in the high-rate stage of the process (Ahn et al.  
336 2011; Jiang et al. 2011). Our results are in agreement and highlight the highest methane  
337 emission at the end of this phase (from day 6 to day 12 of process) coinciding with a  
338 slight decrease of temperature. Around the 12<sup>th</sup> day of process, the CH<sub>4</sub> emission  
339 decreased as well as the temperature and OUR. Chadwich et al. (2011) confirmed that  
340 above 20 °C there exists an exponential correlation between temperature and CH<sub>4</sub>  
341 emissions.

342 The final cumulative results showed that the cyclic aeration favored the CH<sub>4</sub>  
343 emissions. It was expected since this strategy required lower air consumption  
344 (equivalent airflow 1 L min<sup>-1</sup>, Table 2) and an oscillating aeration regime that led to  
345 oxygen levels below 5% (Fig. 1b). This situation was minimized with the oxygen  
346 controller, since the airflow increased for avoiding oxygen concentrations below 11.5%.  
347 On the contrary, the OUR controller presented the lowest overall CH<sub>4</sub> emission,



348 confirming that this type of control based on the respiration of microorganisms is a good  
349 alternative to minimize methane emissions.

350

### 351 3.3.3. N<sub>2</sub>O evolution

352 Temperature, nitrogen content and aeration rate are parameters strongly related  
353 to the N<sub>2</sub>O generation (Hellebrand and Kalk, 2001). Many authors have described that  
354 the highest N<sub>2</sub>O emissions are detected during the initial step (He et al., 2001; El Kader  
355 et al., 2007; Jiang et al., 2011). In fact, in some works, N<sub>2</sub>O was not detected after  
356 starting the process (Fukumoto et al., 2003). In this study, our results showed a  
357 sustained emission of N<sub>2</sub>O along the experimental time, as can be observed in Fig. 2b.  
358 This measure was always among 4 and 6 ppm being the highest values obtained in the  
359 initial stage (first 4-6 d of process). Some studies (He et al., 2001) mentioned that the  
360 temperature could inhibit some mechanisms of N<sub>2</sub>O generation.

361 According to the CH<sub>4</sub> data previously presented, anaerobic conditions were  
362 present with the cyclic aeration. It was confirmed with the N<sub>2</sub>O emissions that were also  
363 higher than those of the other controllers. One possible hypothesis to explain this trend  
364 is that nitrite and nitrate were formed during the high aeration periods and later partially  
365 denitrified to N<sub>2</sub>O during the anoxic-anaerobic periods. Many authors have also related  
366 the N<sub>2</sub>O emissions with the airflow range applied (Willers et al., 1996; Béline et al.,  
367 1999; Loyon et al., 2007). However, no clear relation was observed in this work  
368 between the global airflow supplied and N<sub>2</sub>O emission, which might imply that the key  
369 factor in controlling the N<sub>2</sub>O emissions during composting is the aeration strategy and  
370 the availability of oxygen rather than the amount of oxygen supplied to the reactor.

371

#### 372 3.3.4. NH<sub>3</sub> evolution

373 NH<sub>3</sub> emissions are dependent on C/N ratio, temperature, pH and airflow. All  
374 profiles obtained in our study followed a similar trend to that of temperature curve i.e.,  
375 the highest ammonia emissions appeared during the high-rate thermophilic stage, a  
376 trend that has been demonstrated in previous studies (Pagans et al., 2006). Most NH<sub>3</sub>  
377 concentration values achieved were around 600-700 mg NH<sub>3</sub> m<sup>-3</sup>. Similar ranges were  
378 obtained in bench composting experiments with source-selected OFMSW (Pagans et al.,  
379 2006; Pagans et al., 2007).

380 The cumulative emissions of ammonia are presented in Fig. 2c. NH<sub>3</sub> emissions  
381 were always produced after reaching an alkaline pH. In the cyclic aeration this did not  
382 occur until the fifth day. This strategy provided the highest cumulative NH<sub>3</sub> emission,  
383 68% higher than that detected with the OUR controller, probably because of a longer  
384 thermophilic stage. With the oxygen controller the global emission was similar to that  
385 of the OUR controller. Additionally, other experiments performed with the OUR  
386 controller but using a higher airflow range (between 2 and 3 L min<sup>-1</sup>) showed a  
387 proportional relationship between airflow and NH<sub>3</sub> emission (data not shown).

388

#### 389 3.3.5. Global emissions

390 Table 3 shows the global emissions of CH<sub>4</sub>, N<sub>2</sub>O and NH<sub>3</sub> generated during each  
391 experiment. These values are presented as a function of the weight of waste treated (E)  
392 and are also expressed taking into account the DRI reduction according to the new  
393 functional unit (RIE) proposed by Colón et al. (2012), which allows the results to be  
394 related to the effectiveness of the composting performance. In our case, these units  
395 emphasized the good results that the OUR controller offers since this system led to the

396 highest DRI reduction. All results demonstrated that the OUR controller reduced the  
397 GHG emissions and thus, the environmental impact associated to the composting  
398 process. Actually, the most relevant fact observed was the gradual evolution of the  
399 gaseous emissions detected under the OUR controller. This is crucial aspect to design  
400 and simplify the configuration of gas exhaust treatment technologies typically used in  
401 composting (biofilters, scrubbers, etc.) ant to permit this units to operate in a steady  
402 non-oscillating profile of the gaseous treatment. Specifically, the gradual airflow  
403 evolution and pollutant concentrations would avoid the high emissions observed when  
404 the high sudden airflows appear in the other controllers tested. On the contrary, cyclic  
405 aeration always presented the highest emissions. Similar differences among controllers  
406 were observed using the RIE units.

407         The overall N<sub>2</sub>O emissions values obtained were lower than the data reported in  
408 literature (Amlinger et al., 2008). In the case of methane, similar emissions have been  
409 detected by other authors. Instead, NH<sub>3</sub> emissions were somewhat higher than the  
410 ranges reported in literature although these values could be included within the range  
411 described by Clemens and Culhs (2003) in mechanical-biological treatment facilities  
412 ranging from 0.02 to 1.15 kg NH<sub>3</sub> Mg<sup>-1</sup> OFMSW. According to a recent study (Puyuelo  
413 et al., 2011), these high emissions could be attributed to an estimation of C/N ratio  
414 based on TOC rather than biodegradable organic carbon.

415         From a GHG point of view the results showed again that the OUR controller  
416 significantly decreased this impact. Global data were 7.2, 9.7 and 4.9 kg CO<sub>2</sub>-eq Mg<sup>-1</sup>  
417 OFMSW for oxygen feedback, cyclic and OUR controller, respectively (Table 3).

418 Unfortunately, the contribution of N<sub>2</sub>O emission on the GWP of the oxygen controller  
419 had to be estimated, since this measure could only be undertaken during the first five

420 experimental days due to technical problems. Specifically, a linear extrapolation was  
421 assumed to estimate the global N<sub>2</sub>O emission after 20 days with the oxygen controller.

422 Finally, GWP minimization is even more relevant if data are related to DRI  
423 efficiency (Table 3). Accordingly, it is evident that the OUR controller is a positive  
424 strategy to reduce greenhouse emissions with a parallel reduction of DRI, showing that  
425 a high stabilization of organic matter in high-rate forced-aerated composting is  
426 compatible with a low GWP.

427

#### 428 **4. Conclusions**

429 We have demonstrated that the application of a new advanced controller based  
430 on the on-line determination of the respiration of the composting mass minimizes the  
431 GHG emissions from the composting of biowaste and increases stability of the final  
432 product. This has important effects on the environmental impact related to the  
433 composting process as well as in the design of exhaust gas treatment units for biowaste  
434 composting, a point with relevant implications in the composting acceptance and  
435 development. Further studies should be focused on the application of the OUR  
436 controller to other wastes where composting is the main treatment alternative.

437

#### 438 **Acknowledgments**

439 Authors thank the financial support of the Spanish Ministerio de Economía y Competitividad (Project  
440 CTM 2012-33663).

441

442 **References**

- 443 Adani, F., Ubbiali, P., Genevini, P., 2006. The determination of biological stability of  
444 composts using the dynamic respiration index: The results of experience after  
445 two years. *Waste Manage.* 26, 41-48.
- 446 Ahn, H.K., Mulbry, W., White, J.W., Kondrad, S.L., 2011. Pile mixing increases  
447 greenhouse gas emissions during composting of dairy manure. *Bioresource*  
448 *Technol.* 102, 2904-2909.
- 449 Amlinger, F., Peyr, S., Cuhls, C., 2008. Greenhouse gas emissions from composting and  
450 mechanical biological treatment. *Waste Manage.Res.* 26, 47-60.
- 451 Béline, F., Martinez, J., Chadwick, D., Guiziou, F., Coste, C.M., 1999. Factors affecting  
452 nitrogen transformations and related nitrous oxide emissions from aerobically  
453 treated piggery slurry. *J. Agri. Res.* 73, 235-243.
- 454 Chadwick, D., Sommer, S., Thorman, R., Fanguero, D., Cardenas, L., Amon, B.,  
455 Misselbrook, T., 2011. Manure management: Implications for greenhouse gas  
456 emissions. *Animal Feed Sci. Technol.* 166, 514-531.
- 457 Clemens, J., Cuhls, C., 2003. Greenhouse gas emissions from mechanical and biological  
458 waste treatment of municipal waste. *Environ. Technol.* 24, 745-754.
- 459 Colón, J., Cadena, E., Pognani, M., Barrena, R., Sánchez, A., Font, X., Artola, A., 2012.  
460 Determination of the energy and environmental burdens associated with the  
461 biological treatment of source-separated municipal solid wastes. *Energy*  
462 *Environ. Sci.* 5, 5731-5741.
- 463 de Guardia, A., Petiot, C., Rogeau, D., 2008. Influence of aeration rate and  
464 biodegradability fractionation on composting kinetics. *Waste Manage.* 28, 73-  
465 84.

466 El Kader, N.A., Robin, P., Paillat, J.M., Leterme, P., 2007. Turning, compacting and the  
467 addition of wáter as factors affecting gaseous emissions in farm manure  
468 composting. *Bioresource Technol.* 98, 2619-2628.

469 Fukumoto, Y., Osada, T., Hanajima, D., Haga, K., 2003. Patterns and quantities of NH<sub>3</sub>,  
470 N<sub>2</sub>O and CH<sub>4</sub> emissions during swine manure composting without forced  
471 aeration-effect of compost pile scale. *Bioresource Technol.* 89, 109-114.

472 Guinée, J.B., 2001. Life Cycle Assessment: An Operational Guide To The ISO  
473 Standards. Part 1 And 2. Ministry of Housing. Spatial Planning and Environment  
474 (VROM) and Centre of Environmental Science (CML), Den Haag, The  
475 Netherlands.

476 Giusti, E., Marsili-Libelli, S., 2010. Fuzzy modelling of the composting process.  
477 *Environ. Model. Soft.* 25, 641-647.

478 Haug, R.T., 1993. *The Practical Handbook of Compost Engineering*. Lewis Publishers,  
479 Boca Raton, FL.

480 He, Y., Inamori, Y., Mizuochi, M., Kong, H., Iwami, N., Sun, T., 2001. Nitrous oxide  
481 emissions from aerated composting of organic waste. *Environ. Sci. Technol.* 35,  
482 2347-2351.

483 Hellebrand, H.J., Kalk, W.D., 2001. Emission of methane, nitrous oxide, and ammonia  
484 from dung windrows. *Nutr. Cycl. Agroecosys.* 60, 83-87.

485 Jiang, T., Schhardt, F., Li, G., Gou, R., Zhao, Y., 2011. Effect of C/N ratio, aeration  
486 rate and moisture content on ammonia and greenhouse gas emission during the  
487 composting. *J. Environ. Sci.* 23, 1754-1760.

488 Keener, H. M., Elwell, D.L., Ekince, K., Hoitink, H.A.J., 2001. Composting and value-  
489 added utilization of manure from a swine finishing facility. *Compost Sci. Util.* 9,  
490 312-321.

491 Kim, S., Deshusses, M.A., 2008. Determination of mass transfer coefficients for  
492 packing materials used in biofilters and biotrickling filters for air pollution  
493 control. *Chem. Eng. Sci.* 63, 841-855.

494 IPCC, 2006. International Panel on Climate Change. IPCC Guidelines for National  
495 Greenhouse Gas Inventories: Workbook, International Panel on Climate Change,  
496 Hayama, Kanagawa.

497 Loyon, L., Guiziou, F., Béline, F., Peu, P., 2007. Gaseous emissions (NH<sub>3</sub>, N<sub>2</sub>O, CH<sub>4</sub>  
498 and CO<sub>2</sub>) from the aerobic treatment of piggery slurry-comparison with a  
499 conventional storage system. *Biosyst. Eng.* 97, 472-480.

500 Osada, T., Kuroda, K., Yonaga, M., 2000. Determination of nitrous oxide, methane, and  
501 ammonia emissions from a swine waste composting process. *J. Mat. Cycl. Waste*  
502 *Manage.* 2, 51-56.

503 Pagans, E., Barrena, R., Font, X., Sánchez, A., 2006. Ammonia emissions from the  
504 composting of different organic wastes. Dependency on process  
505 temperature. *Chemosphere* 62, 1534-1542.

506 Pagans, E., Font, X., Sánchez, A., 2007. Coupling composting and biofiltration for  
507 ammonia and volatile organic compounds removal. *Biosyst. Eng.* 97, 491-500  
508 (2007).

509 Papadimitriou E.K., Bidlingmaier, W., Gea, T., 2010. Fundamentals in selecting input  
510 and output variables for composting process automatic controllers. *Compost Sci.*  
511 *Util.* 18, 6-21.

512 Pognani, M., Barrena, R., Font, X., Adani, F., Scaglia, B., Sánchez, A., 2011. Evolution  
513 of organic matter in a full-scale composting plant for the treatment of sewage  
514 sludge and biowaste by respiration techniques and pyrolysis-GC/MS.  
515 *Bioresource Technol.* 102, 4536-4543.

516 Ponsá, S., Gea, T., Sánchez, A., 2010. Different indices to express biodegradability in  
517 organic solid wastes. *J. Environ. Qual.* 39, 706-712.

518 Puyuelo, B., Gea, T., Sánchez, A., 2010. A new control strategy for the composting  
519 process based on the oxygen uptake rate. *Chem. Eng. J.* 165, 161-169.

520 Puyuelo, B., Ponsá, S., Gea, T., Sánchez, A., 2011. Determining C/N ratios for typical  
521 organic wastes using biodegradable fractions. *Chemosphere* 85, 653-659.

522 Ruggieri, L., Gea, T., Monpeó, M., Sayara, T., Sánchez, A., 2008. Performance of  
523 different systems for the composting of the source-selected organic fraction of  
524 municipal solid waste. *Biosyst. Eng.* 101, 78-86.

525 Ruggieri, L., Gea, T., Artola, A., Sánchez, A., 2009. Air filled porosity measurements  
526 by air pycnometry in the composting process: a review and a correlation  
527 analysis. *Bioresource Technol.* 100, 2655-2666.

528 Scaglia, B., Orzi, V., Artola, A., Font, X., Sánchez, A., Adani, F., 2011. Odours and  
529 volatile organic compounds emitted from municipal solid waste at different  
530 stage of decomposition and relationship with biological stability. *Bioresource*  
531 *Technol.* 102, 4638-4645.

532 Shen, Y., Ren, L., Li, G., Chen, T., Guo, R., 2011. Influence of aeration on CH<sub>4</sub>, N<sub>2</sub>O  
533 and NH<sub>3</sub> emissions during aerobic composting of a chicken manure and high  
534 C/N waste mixtures. *Waste Manage.* 31, 33-38.



535 Smet, E., Van Langenhove, H., De Bo, I., 1999. The emission of volatile compounds  
536 during the aerobic and the combined anaerobic/aerobic composting of biowaste.  
537 Atmos. Environ. 33, 1295-1303.

538 The US Department of Agriculture and The US Composting Council, 2001. Test  
539 Methods for the Examination of Composting and Compost, Edaphos  
540 International, Houston.

541 Willers, H.C., Derikx, P.J.L., ten Have, P.J.W., Vijn, T.K., 1996. Emission of ammonia  
542 and nitrous oxide from aerobic treatment of veal calf slurry. J. Agri. Eng. Res.  
543 63, 345-352.

544

545 **Tables**

546

547 **Table 1.** Characterization of the initial OFMSW collected and final products obtained  
548 after 20 experimental days using each specific airflow control system.

549

550

<b>Material</b>		Dry Matter (%, wb)	Organic Matter (%, db)	Organic Carbon (%, db)	Total Nitrogen (%, db)
<b>Initial OFMSW</b>		33.5 ± 0.3	78 ± 2	43.3	2.05 ± 0.07
<b>Final Product</b>	Oxygen control	31.0 ± 0.3	74 ± 3	41.0	2.1 ± 0.1
	Cyclic control	26.6 ± 0.5	77 ± 3	43.0	2.36 ± 0.05
	OUR control	44.0 ± 0.9	74 ± 3	41.0	2.4 ± 0.1

551

552 OFMSW: Organic Fraction of Municipal Solid Waste; wb: wet basis; db: dry basis.

553

554

555 **Table 2.** Principal parameters evaluated for each aerated system.

556

557

558

<b>Aeration system</b>	Energy consumption (kJ Mg <sup>-1</sup> OFMSW)	OUR <sub>max</sub> (g O <sub>2</sub> h <sup>-1</sup> )	Final DRI (mg O <sub>2</sub> g <sup>-1</sup> OM h <sup>-1</sup> )
Oxygen control	548 ± 32	15.1 ± 0.6	2.1 ± 0.05
Cyclic control	487 ± 67	-	1.9 ± 0.07
OUR control	634± 24	13.0 ± 0.3	1.5 ± 0.06

559

560 OUR<sub>max</sub>: maximum oxygen uptake rate reached; DRI: dynamic respiration index average.

561

562

563 **Table 3.** Total emissions of CH<sub>4</sub>, N<sub>2</sub>O and NH<sub>3</sub> and total global warming potential for  
 564 the three systems considered.

565

566

<b>Global emissions and impact</b>	CH <sub>4</sub> emissions kg CH <sub>4</sub> Mg <sup>-1</sup> OFMSW	N <sub>2</sub> O emissions kg N <sub>2</sub> O Mg <sup>-1</sup> OFMSW	NH <sub>3</sub> emissions kg NH <sub>3</sub> Mg <sup>-1</sup> OFMSW	Global warming potential kg CO <sub>2</sub> -eq
Oxygen control	0.12±0.02	> 0.0040	> 0.7	7.2±0.5
Cyclic control	0.25±0.03	0.0152±0.005	> 1.0	9.7±0.9
OUR control	0.07±0.01	0.0094±0.001	0.7±0.01	4.5±0.3
<b>RIE<sub>e</sub></b>	kg CH <sub>4</sub> Mg <sup>-1</sup> OFMSW DRI <sub>red</sub> <sup>-1</sup>	kg N <sub>2</sub> O Mg <sup>-1</sup> OFMSW DRI <sub>red</sub> <sup>-1</sup>	kg NH <sub>3</sub> Mg <sup>-1</sup> OFMSW DRI <sub>red</sub> <sup>-1</sup>	kg CO <sub>2</sub> -eq DRI <sub>red</sub> <sup>-1</sup>
Oxygen control	0.029±0.002	> 0.0011	> 0.18	2.21±0.05
Cyclic control	0.060±0.004	0.0043	> 0.29	2.98±0.09
OUR control	0.020±0.001	> 0.0005	0.18±0.02	1.32±0.03

567

568

569

570

571

572

573

574

OFMSW: Organic fraction of municipal solid waste; OUR: oxygen uptake rate; DRI: dynamic respiration index average.  $DRI_{red} = (DRI_{initial} - DRI_{final})$ : Dynamic respiration index reduction during the experimental process; RIE<sub>ec</sub>: Respiration index efficiency for global emissions; RIE<sub>ec</sub>: Respiration index efficiency for global emissions.

575 **Legends to Figures**

576 **Figure 1.** Evolution of temperature and airflow applied for the three aeration strategies studied  
577 (one replication shown as example): oxygen feedback controller (a), cyclic controller (b) and  
578 OUR controller (c). The OUR profile is also showed in the experiment C and during the high-  
579 rate decomposition stage of the case A. Oxygen profile is shown for cyclic controller.

580 **Figure 2.** Cumulative emission of CH<sub>4</sub> (a), N<sub>2</sub>O (b) and NH<sub>3</sub> (c) for the oxygen, cyclic and  
581 OUR controller (one replication shown as example). N<sub>2</sub>O emission for the oxygen controller  
582 could only be measured during the first five experimental days due to technical  
583 problems.

584

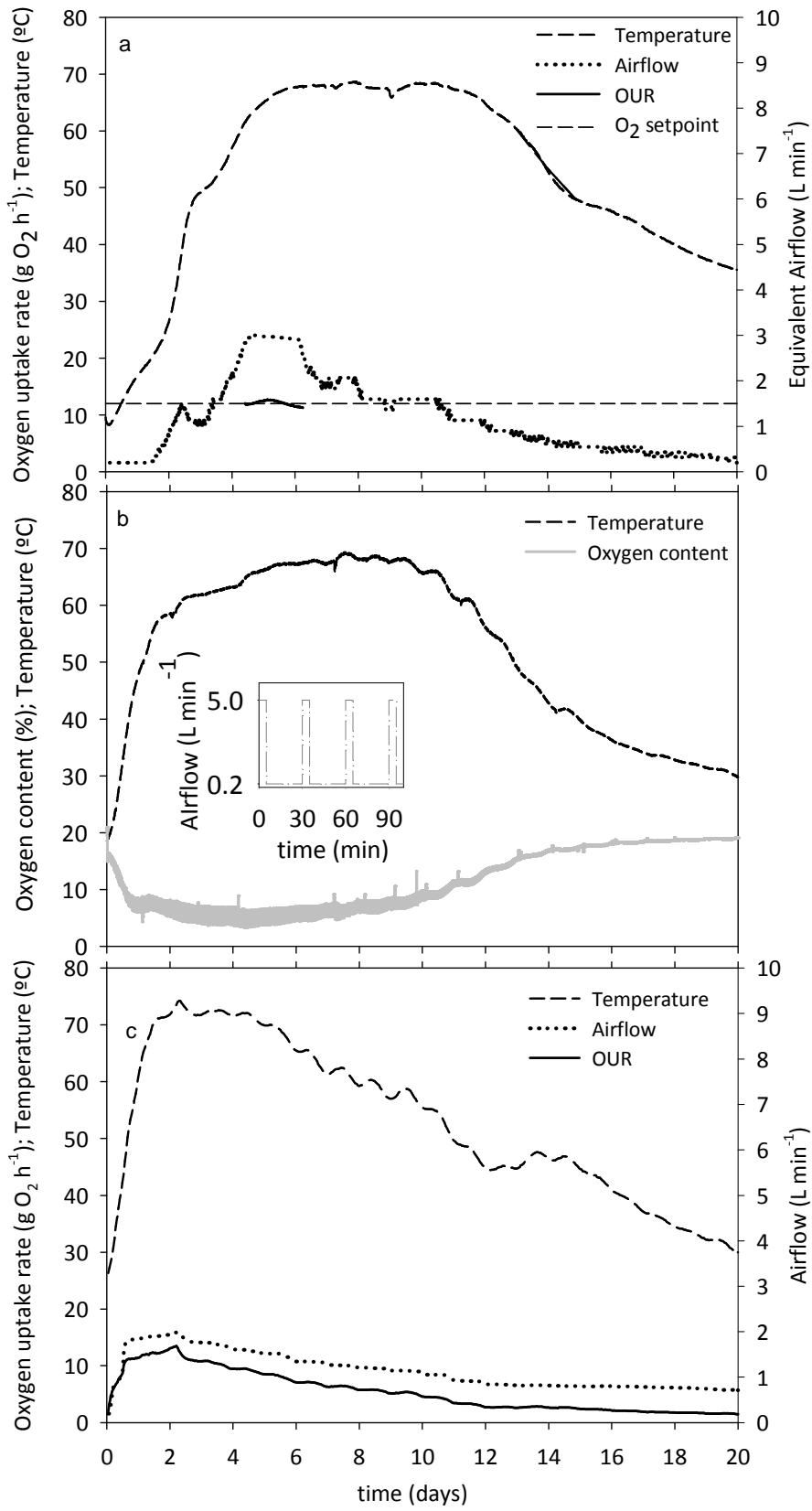
585

586

587

588

589 **Fig. 1**



590

591

592 **Fig. 2**

593

594

